Supplementary Figures

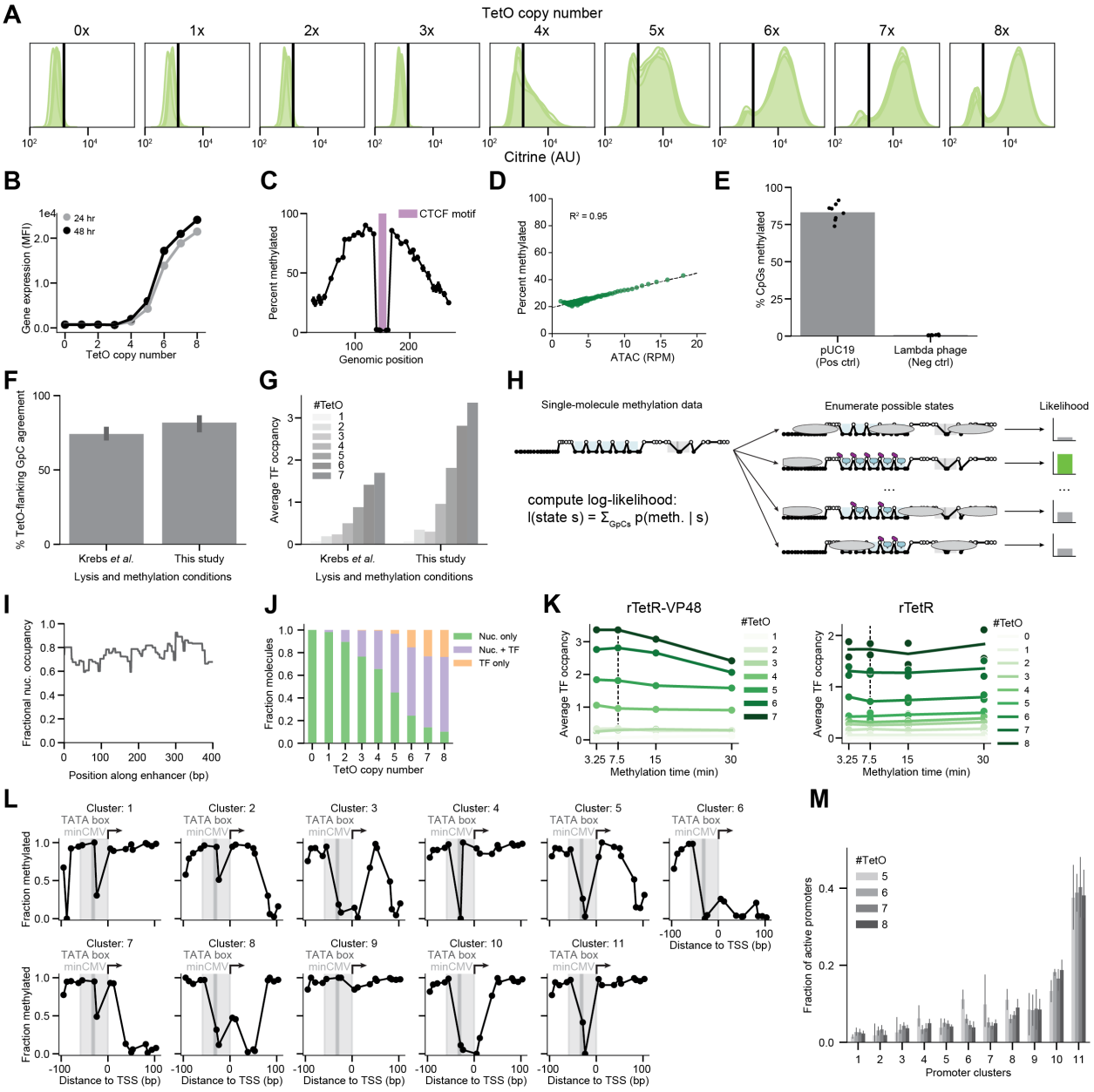

Figure S1

A) Flow cytometry distributions for Citrine fluorescence for the 0-8xTetO amplicons. Data are from 2-4 technical replicates.

B) MFI for Citrine fluorescence for the 0x-8xTetO amplicons at 24 and 48 hours.

C) Average methylation signal around a synthetic amplicon containing a single CTCF site (location marked in purple). Error bars represent the 95% CI from 3 biological replicates.

D) Relationship between the average ATAC-seq signal (RPM) and average methylation probability from SMF for all ATAC-seq peaks genome-wide grouped into 100 quantile bins.

E) Methylation probabilities at CpGs from the fully methylated (pUC19) and fully unmethylated (Lambda phage) EM-seq controls. Each dot represents an experiment and the bar represents the average.

F) The percent of pairs of GpCs that flank the same TetO site that have the same methylation status on the same molecule. Error bars represent the 95% CI obtained by combining data across all pairs of GpCs that flank all TetO sites.
G) Average TF occupancy across 0x-8xTetO amplicons under different lysis and methylation conditions.
H) Cartoon schematic of the probabilistic binding model. For each observed single-molecule methylation signal, we enumerate all possible underlying molecular configurations of TFs and nucleosomes and assign each a likelihood of being observed. We then select the state with the maximum likelihood.
I) The fraction of molecules with a nucleosome overlapping each position in the synthetic enhancer sequence.
J) The fraction of molecules which have enhancers either a) completely covered by nucleosomes, b) only bound by TFs, or c) covered with a mix of the two as a function of the number of TetO sites.
K) Average TF occupancy across all amplicons for both rTetR-VP48 and rTetR alone as a function of the duration of the methylation reaction. Dotted line represents the conditions used in our assay (7.5 min).
L) Average methylation signal across the promoter region for molecules grouped into each of the 11 k-means clusters of “active” (nucleosome-free) promoters.
M) Fraction of “active” (nucleosome-free) promoters that are found in each k-means cluster, faceted by the number of TetO sites in the amplicon. Error bars represent the 95% CI from 4 biological replicates. Cluster numbers are the same as in (L).

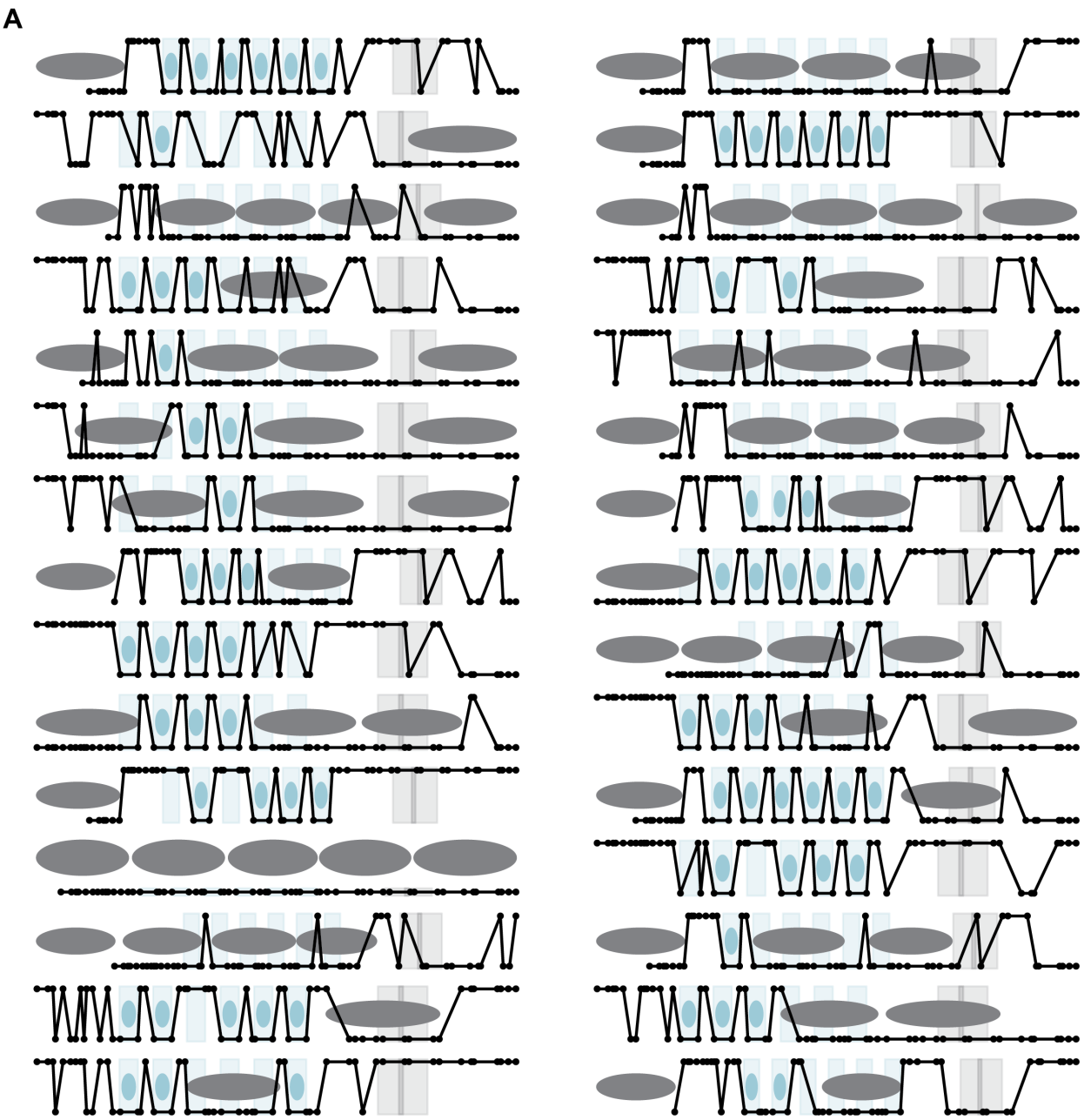

Figure S2

A) Exemplar data for 30 random single molecules, each of 6xTetO background 0, after 24 hours of dox induction (1,000 ng/ml) and binding model calls for nucleosomes (gray) and rTetR-VP48 (blue). For each molecule, points on the top are methylated (accessible) and points on the bottom are unmethylated (inaccessible).

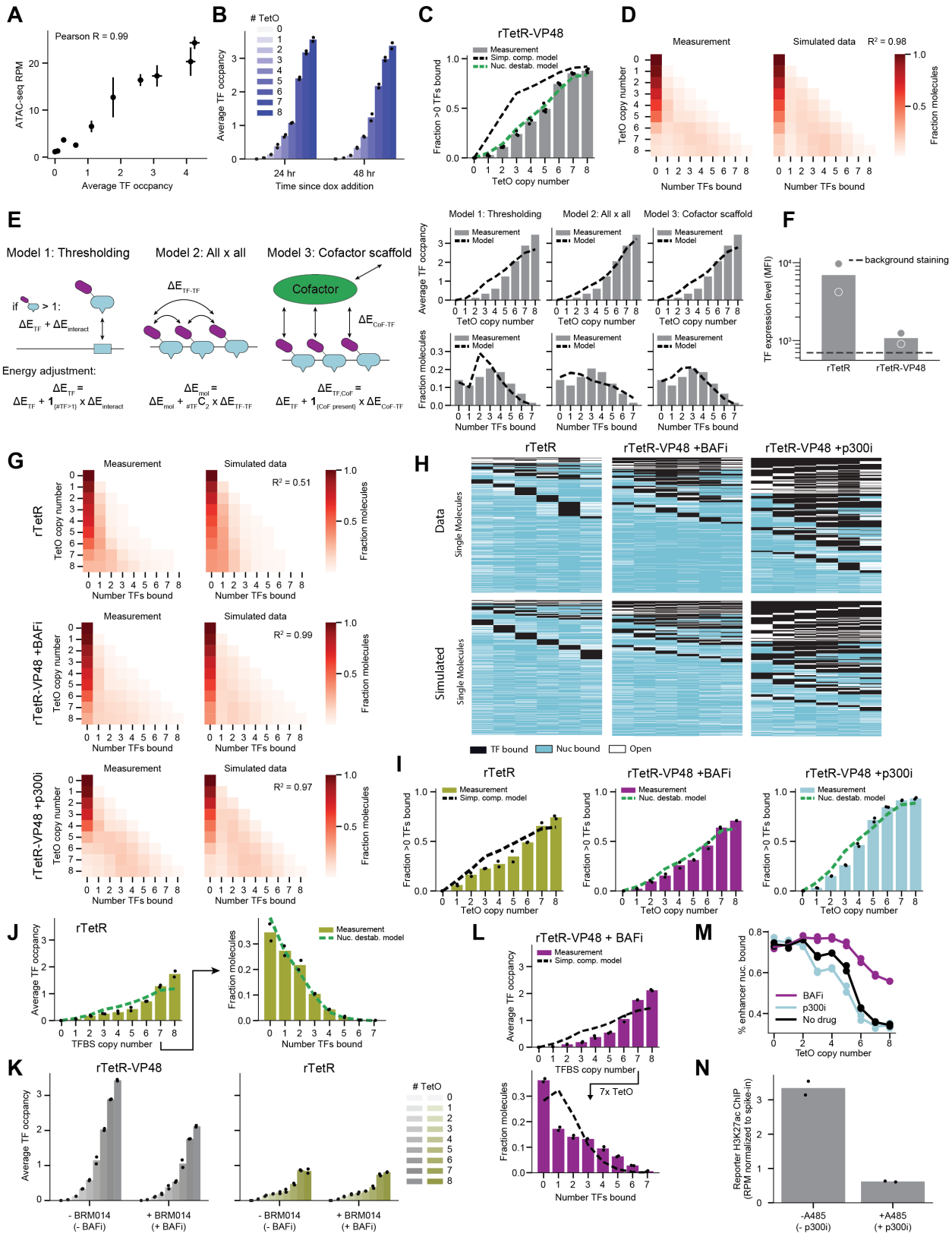

Figure S3

A) Relationship between average TF occupancy and ATAC-seq signal (RPM) for a selection of single enhancer amplicons from multiple backgrounds. Each dot represents a single enhancer. Error bars represent the 95% CI from 4 (SMF) or 2 (ATAC-seq) biological replicates.
B) Average TF occupancy across 0x-8xTetO amplicons at 24 and 48 hours.
C) Observed fraction of molecules with >0 TFs bound for enhancers with increasing number of TetO sites (four biological replicates) fit to either the Simple Competition (r^2 = 0.44) or Nucleosome Destabilization (r^2 = 0.99) models (from **Fig. 2D-E**).
D) Observed occupancy distributions across all enhancers (left) with matching simulations from the Nucleosome Destabilization model (right). Each row represents a single enhancer and each column represents the number of TFs bound. The pixel intensity at (row i, column j) indicates the fraction of molecules with i TetO sites that have j TFs bound. Rows sum to 1.
E) Three alternate TF cooperativity models (see Methods). Cartoons demonstrating how the TF cooperativity models are encoded (left) and fits to average occupancy and occupancy distribution data (right).
F) Flow cytometry for FLAG-tagged TF expression for cells expressing rTetR or rTetR-VP48. Dotted line represents the level of background staining. Data are from two biological replicates.
G) Observed occupancy distributions across all enhancers (left) with matching simulations from the Nucleosome Destabilization model (right) as in (D) for rTetR only, rTetR-VP48 treated with BAF inhibitor, and rTetR-VP48 treated with p300 inhibitor.
H) Full molecular state representations for 10,000 measured (top) or simulated (bottom) molecules (as in **Fig. 2G**) for rTetR only, rTetR-VP48 treated with BAF inhibitor, and rTetR-VP48 treated with p300 inhibitor. Each column represents a TetO site and each row represents a molecule. Sites are colored by their occupancy status.
I) Observed fraction of molecules with >0 TFs bound as in (C) for rTetR only, rTetR-VP48 treated with BAF inhibitor, and rTetR-VP48 treated with p300 inhibitor. Fits are either to the Simple Competition (rTetR only) or Nucleosome Destabilization (rTetR-VP48 + inhibitors) models (r^2 = 0.86, 0.96, and 0.96, respectively). Data are from two biological replicates.
J) Observed average occupancy (left) and occupancy distribution (right) of rTetR (two biological replicates) with a fit from the Nucleosome Displacement model (r^2 = 0.83 and 0.96, respectively) (cf. **Fig. 2J-K**).
K) Average TF occupancy across 0x-8xTetO amplicons for rTetR-VP48 (left) and rTetR only (right) with and without treatment with BAF inhibitor. Data are from two biological replicates.
L) Observed average occupancy (top) and occupancy distribution (bottom) of rTetR-VP48 in the presence of the BAF inhibitor BRM014 (two biological replicates) with a fit from the Simple Competition model (r^2 = 0.78 and 0.51, respectively) (cf. **Fig. 2L-M**).
M) Observed fraction of molecules with nucleosomes overlapping the enhancer as a function of the number of TetO sites for rTetR-VP48, rTetR-VP48 treated with BAF inhibitor, and rTetR-VP48 treated with p300 inhibitor.
N) Average H3K27ac signal across the synthetic reporter locus with and without p300 inhibition. Data are from two biological replicates, and the signal is normalized to spike-in mouse chromatin.

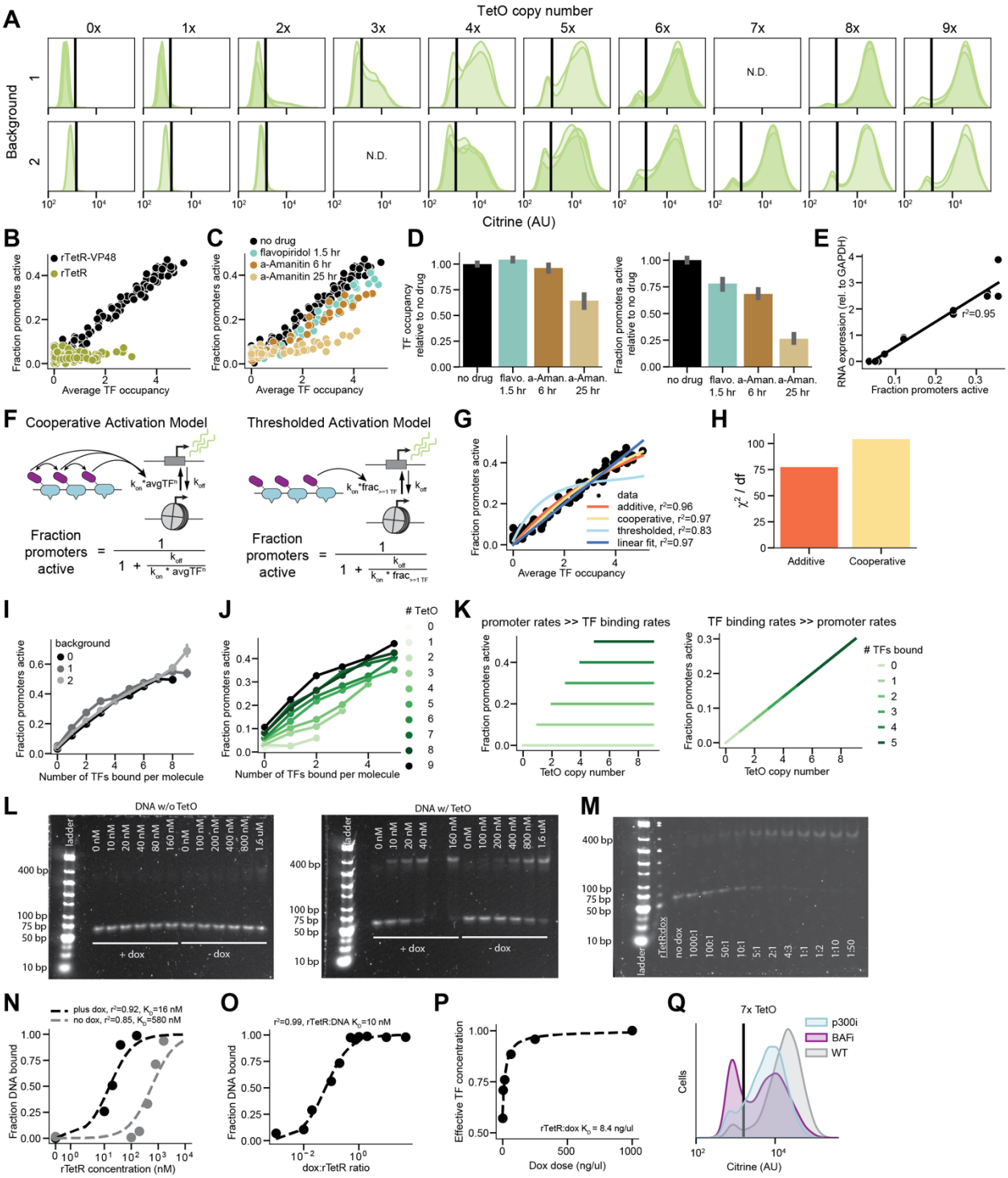

Figure S4

A) Flow cytometry distributions for the 0-9xTetO amplicons in backgrounds 1 and 2. Data are from 2-4 technical replicates.

B) Relationship between rTetR-VP48 (black) and rTetR (green) occupancy and the fraction of active promoters.

C) Relationship between rTetR-VP48 occupancy and the fraction of active promoters without drugs (black) and across transcription inhibition conditions with 24 hours of dox: flavopiridol for 1.5 hours (cyan) and alpha-amanitin for 6 hours (brown), alpha-amanitin for 25 hours (tan).

D) Quantification of C for TF occupancy (left) and fraction of promoters active (right) across transcription inhibition conditions relative to no drug treatment for 5x-8xTetO. Alpha-amanitin for 25 hours (tan) likely reduces rTetR-VP48 concentration due to global reduction of transcription.
E) Relationship between fraction of promoters active and RNA expression (measured by RT-qPCR, normalized to GAPDH levels) on 0-8xTetO with two technical replicates each. Black line is a linear fit.
F) Schematics of alternative models relating TF binding to promoter activation. Cooperative Activation (left) assumes activation is cooperative with the number of TFs bound on average (k_{on}*avgTF^n). Thresholded Activation (right) assumes activation of the promoter occurs when there is at least 1 TF present (k_{on}*$frac_{>=1\ TF}$).
G) Model fits for additional models in F on the relationship between average rTetR-VP48 occupancy and fraction of promoters active. Fit parameters for cooperative model: k_{on}/k_{off} = 0.13 ± 0.006 TF^{-1}, n = 1.1 ± 0.04. Fit parameter for thresholded model: k_{on}/k_{off} = 0.5 ± 0.1.
H) Chi-squared per degree of freedom comparing Additive and Cooperative Activation model fits in C.
I) Instantaneous relationship between the number of rTetR-VP48s bound and the promoter state on the same molecule for all TetO copy numbers across backgrounds.
J) Instantaneous relationship between the number of rTetR-VP48s bound (up to 9) and the promoter state on the same molecule separating molecules by TetO copy number.
K) Example plots to compare to data in **Fig. 3H** representing the expected relationship between TetO copy number, number of TFs bound, and promoter activity on the same molecules if promoter rates are much faster than TF binding rates (left) or vice versa (right).
L) EMSA of rTetR (concentration noted above each lane) binding to 60 bp target DNA (1 nM) without a TetO site (left) and with a TetO site (right) in the presence and absence of doxycycline (1:50 rTetR to dox concentration).
M) EMSA of rTetR (160 nM) binding to 60 bp target DNA (1 nM) with a TetO site across varying dox concentrations (ratio relative to rTetR concentration noted under each lane) (left).
N) Quantification of EMSA gel with TetO sites in L in the presence (black) and absence (gray) of dox with binding isotherm fits ($y=x/(K_D+x)$).
O) Quantification of EMSA gel in M with binding isotherm fit ($y=x/(K_D+x)$) where K_D is the affinity of rTetR to DNA and the affinity of dox to rTetR is assumed to be much smaller.
P) Quantification of the apparent TF concentration from relative *in vivo* rTetR-VP48 concentration (from binding energy in Nucleosome Destabilization model) across dox concentrations with binding isotherm fit.
Q) Flow cytometry distributions for a 7xTetO reporter cell line without drugs (gray), under p300 inhibition (cyan) and under BAF inhibition (purple) after 24 hours of dox induction.

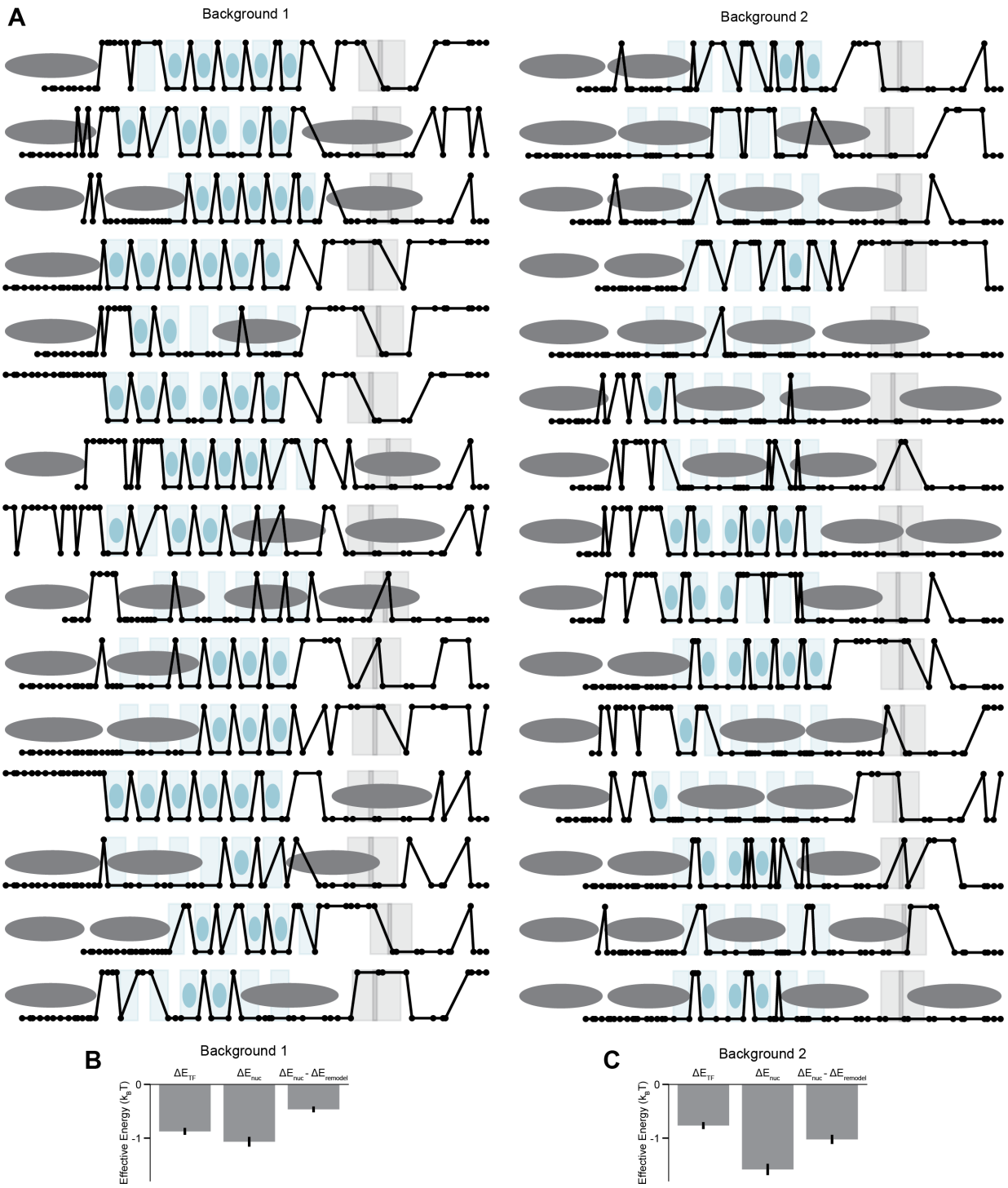

Figure S5

A) Exemplar data for 15 random single molecules, each of 6xTetO background 1 (left) and background 2 (right), 24 hours after dox induction (1000 ng/ml) and binding model calls for nucleosomes (gray) and rTetR-VP48 (blue). For each molecule, points on the top are methylated (accessible) and points on the bottom are unmethylated (protected). B-C) Model parameters for the equilibrium partition function model fit on background 1 and 2 molecules, respectively.

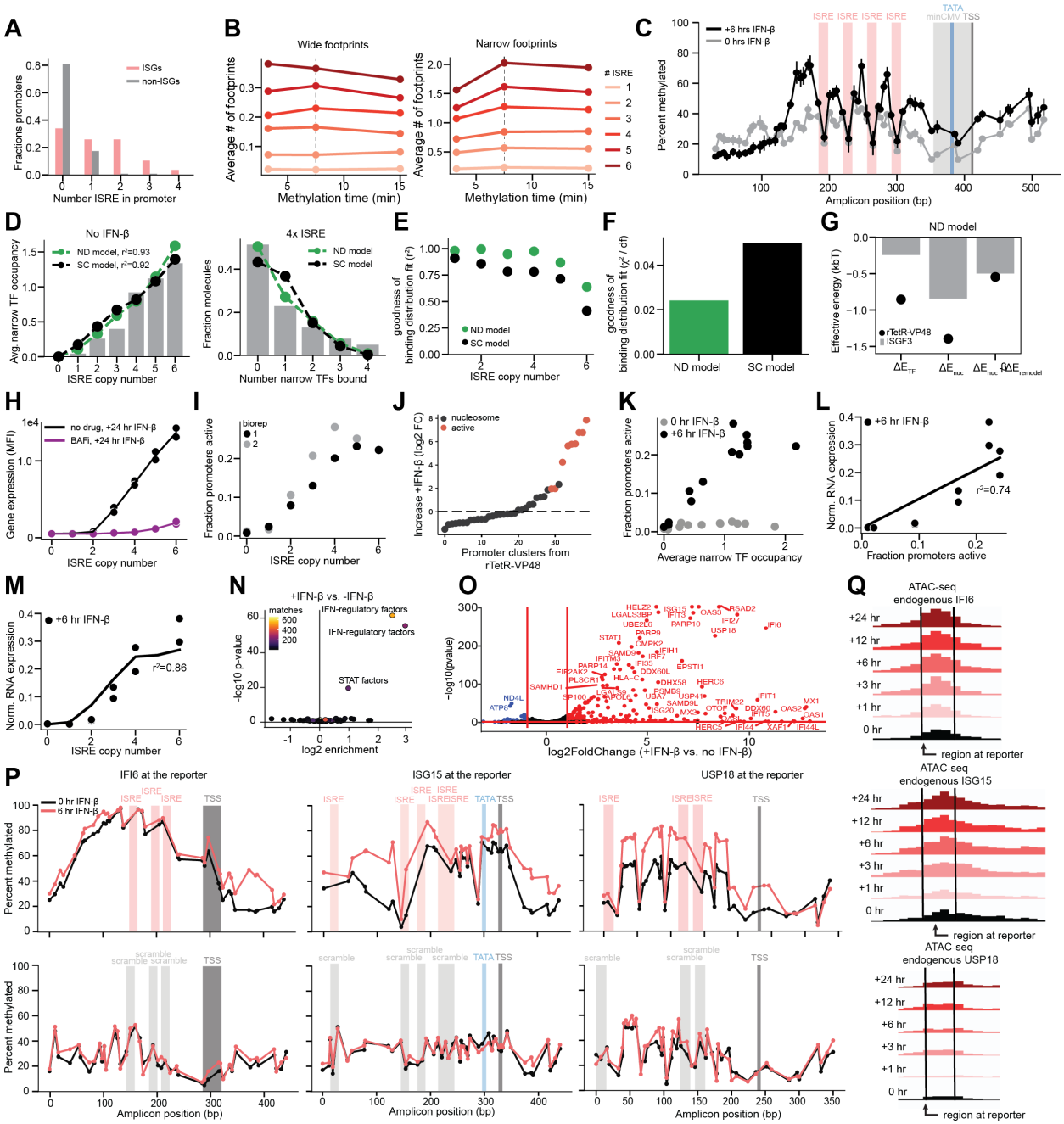

Figure S6

A) Distributions of the number of ISREs within a 500 base pair window around TSSs of ISGs identified from bulk RNA-seq (pink) and of non-ISGs (gray).

B) Relationship between methylation time and measured average occupancy across amplicons after 24 hours of IFN-β stimulation for wide footprints (left) and narrow footprints (right). Dashed black line is the methylation time chosen for all subsequent experiments.

C) Aggregated methylation data obtained for the construct with 4 ISRE sites present, with (black) and without (gray) IFN-β present. Error bars are standard deviation between two biological replicates.

D) Relationship between ISRE copy number and average narrow footprint occupancy for the average of two biological replicates (left) and the distribution of narrow footprints bound for 4x ISRE sites (right) prior to stimulation fit

by the Simple Competition model (black) and Nucleosome Displacement model (green). For both models, the nucleosome energy is fit to the nucleosome value measured in rTetR-VP48 experiments.
E-F) Goodness of fit of number bound distributions in D by r^2 across ISRE copy numbers (E) and chi-squared per degrees of freedom (F) on the number bound distributions for both models.
G) Fit parameters (averaged across two biological replicates) from Nucleosome Displacement model (gray) in D; black dots are rTetR-VP48 parameters.
H) Relationship between ISRE copy number and gene expression (as measured by flow cytometry at 24 hours of IFN-β stimulation) with (purple) and without (black) BAF inhibition for two technical replicates.
I) Relationship between ISRE copy number and fraction of promoters active across two biological replicates at 6 hours of IFN-β stimulation.
J) Enrichment of active promoter clusters (classified using rTetR-VP48 data) at 6 hours of IFN-β stimulation compared to 0 hours for two biological replicates.
K) Relationship between narrow footprint occupancy and fraction of promoters active with (black) and without (gray) 6 hours of IFN-β stimulation.
L) Relationship between fraction of promoters active and RNA expression (measured by normalized RT-qPCR) on 0-6xISRE for two technical replicates. Black line is a linear fit.
M) Relationship between ISRE copy number and gene expression (as measured by RT-qPCR of Citrine mRNA) for two technical replicates. Black line is the coupled Additive Activation model and linear fit from fraction promoters active to gene expression with input of measured average wide TF occupancy.
N) Differential ATAC-seq chromatin accessibility of TF motif types after 6 hours of IFN-β stimulation over two biological replicates.
O) Differential RNA-seq expression after 6 hours of IFN-β stimulation over two biological replicates.
P) Aggregated methylation data obtained for three reporter constructs with endogenous ISG promoters and proximal enhancers present (IFI6, ISG15, USP18) with intact ISREs (top) and scrambled ISREs (bottom) with (pink) and without (black) IFN-β present.
Q) ATAC-seq tracks of normalized chromatin accessibility to the same scale over an IFN-β stimulation timecourse for IFI6, ISG15, and USP18. Black lines denote the region that was installed at the reporter.

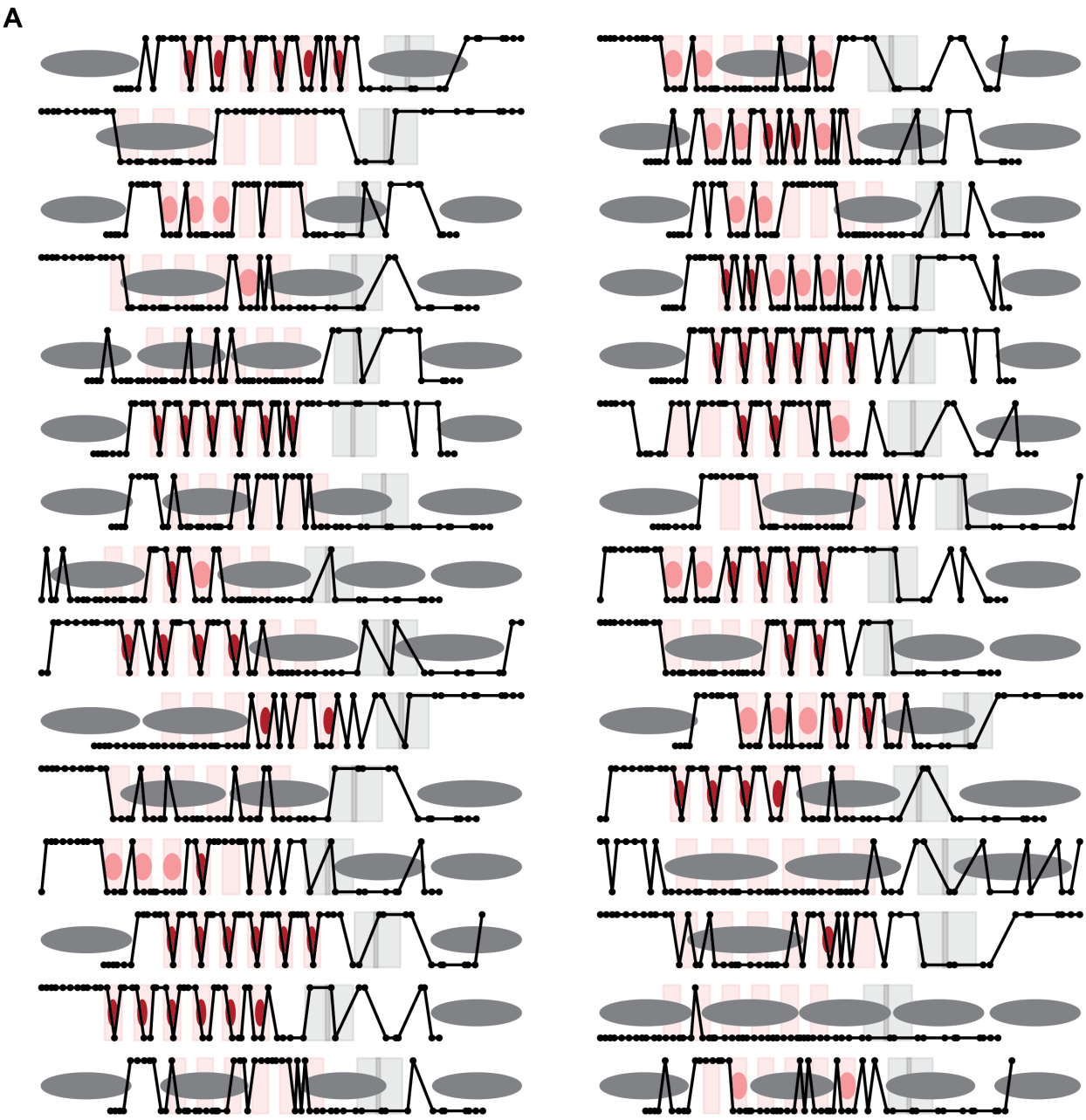

Figure S7

A) Exemplar data for 30 random single molecules, each with 6xISRE, after 6 hours of IFN-β and binding model calls for nucleosomes (gray), narrow footprints (red), and wide footprints (pink). For each molecule, points on the top are methylated (accessible) and points on the bottom are unmethylated (protected).

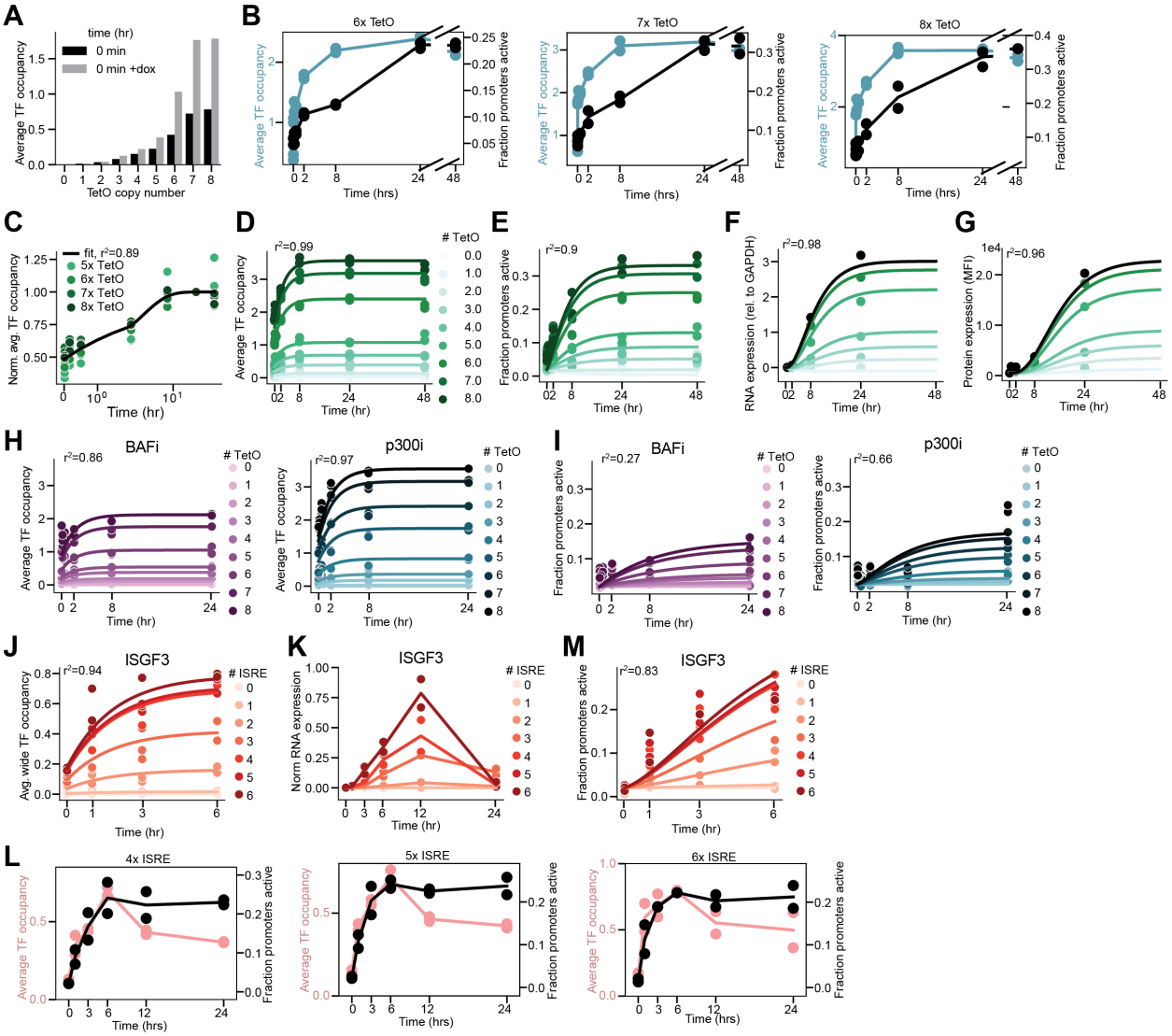

Figure S8

A) rTetR-VP48 occupancy without (black) and with dox (gray) present during sample processing across TetO copy numbers.

B) Representative temporal delay between rTetR-VP48 occupancy (blue) and promoter activation (black) for two biological replicates of 6-8 TetO sites.

C) Fit of single exponential to average rTetR-VP48 occupancy normalized to 48 hour value for two biological replicates of 5-8 TetO sites.

D-G) Average rTetR-VP48 occupancy (D), fraction of promoters active (E), Citrine RNA expression as measured by RT-qPCR (F) and Citrine protein levels as measured by flow cytometry (G) over time for two biological replicates of 0-8 TetO sites. Lines are the fit kinetic model (as described in **Fig. 5D**).

H-I) Average rTetR-VP48 occupancy (H) and fraction of promoters active (I) over time for two biological replicates of BAF inhibition (purple) and p300 inhibition (blue). Lines are the fit kinetic model (as described in **Fig. 5D**).

J) Average wide footprint occupancy over time during the activation process (up to six hours) for two biological replicates of 0-6 ISRE sites. Lines are fit kinetic model (as described in **Fig. 5D**).

K) Citrine RNA expression as measured by normalized RT-qPCR over time for two technical replicates of 0,1,2,3,4, and 6 ISRE sites.

L) Representative lack of temporal delay between wide footprint occupancy (pink) and promoter activation (black) for two biological replicates of 4-6 ISRE sites.

M) Fraction of promoters active over time during the activation process (up to six hours) for two biological replicates of 0-6 ISRE sites. Lines are fit kinetic model (as described in **Fig. 5D**).